Environmental Toxicology and Chemistry—Volume 42, Number 4—pp. 778–792, 2023
Received: 5 July 2022 | Revised: 16 August 2022 | Accepted: 25 January 2023

Environmental Chemistry

Characterization of Gaseous and Particulate Phase Polycyclic Aromatic Hydrocarbons Emitted During Preharvest Burning of Sugar Cane in Different Regions of Kwa-Zulu Natal, South Africa

G. Geldenhuys,[a,b,c] J. Orasche,[d] G. Jakobi,[d] R. Zimmermann,[d,e] and Patricia B. C. Forbes[a,*]

[a]Department of Chemistry, Faculty of Natural and Agricultural Sciences, University of Pretoria, Pretoria, South Africa
[b]Processing Laboratory, Impala Platinum, Rustenburg, South Africa
[c]Skin Rejuvenation Technologies, Irene, South Africa
[d]Joint Mass Spectrometry Centre, Cooperation Group "Comprehensive Molecular Analytics," Helmholtz Zentrum München, Neuherberg, Germany
[e]Joint Mass Spectrometry Centre, Institute of Chemistry, University of Rostock, Rostock, Germany

Abstract: Biomass burning is a significant anthropogenic source of air pollution, including the preharvest burning of sugar cane. These burn events result in atmospheric emissions, including semivolatile organic compounds, that may have adverse impacts on air quality and human health on a local, regional, and even a global scale. Gaseous and particulate polycyclic aromatic hydrocarbon (PAH) emissions from various sugar cane burn events in the province of Kwa-Zulu Natal in South Africa were simultaneously sampled using a portable denuder sampling technology, consisting of a quartz fiber filter sandwiched between two polydimethylsiloxane multichannel traps. Total gas and particle phase PAH concentrations ranged from 0.05 to 9.85 μg m^{-3} per individual burn event, and nine PAHs were quantified. Over 85% of all PAHs were found to exist in the gas phase, with smaller two- and three-ring PAHs, primarily naphthalene, 1-methyl naphthalene, and acenaphthylene, being the most dominant and causing the majority of variance between the burn sites. The PAH profiles differed between the different burn events at different sites, emphasizing the significant influence that the crop variety, prevailing weather conditions, and geographical location has on the type and number of pollutants emitted. The potential carcinogenicity of the PAH exposure was estimated based on toxic equivalency factors that showed varying risk potentials per burn event, with the highest value of 5.97 ng m^{-3}. *Environ Toxicol Chem* 2023;42:778–792. © 2023 The Authors. *Environmental Toxicology and Chemistry* published by Wiley Periodicals LLC on behalf of SETAC.

Keywords: Biomass burning; Denuder; Polycyclic aromatic hydrocarbon; Sugar cane

INTRODUCTION

Sugar cane is an essential commercial crop worldwide; it is extremely versatile, being a rich source of food, fiber, fodder, fertilizer, and numerous valuable byproducts that can be used for human and animal consumption, as well as providing a source of renewable energy (Solomon, 2011). The crop is grown in tropical or subtropical climates, with Brazil producing over 40% of the world total followed by India and China (Flack-Prain et al., 2021; South African Sugar Association [SASA], 2019). The sugar cane industry in South Africa is ranked in the top 15 out of approximately 120 sugar-producing countries worldwide and is one of the world's leading producers of high-quality sugar with an estimated average production of 2.3 million tons/season (SASA, 2019). The industry is varied, combining the agricultural activities of sugar cane farming with the manufacture of raw and refined sugar, syrup, and a range of other by-products (SASA, 2012).

The burning of sugar cane prior to harvest is common practice in South Africa, where over 90% of the sugar cane is burnt (Pryor et al., 2017). The primary reason for burning the sugar cane is economic: most of the excess waste material is eliminated, leading to improved efficiencies of harvesting, handling, and milling. The preharvest burns also chase away the unwanted snakes and cane rats before the workers enter the fields. An alternative to burning prior to harvest is "green

This article includes online-only Supporting Information.

* Address correspondence to patricia.forbes@up.ac.za
Published online 31 January 2023 in Wiley Online Library (wileyonlinelibrary.com).
DOI: 10.1002/etc.5579

harvesting," which involves the cutting of the adult cane stalk, the removal of leaves and unwanted matter, and the covering of the plant's roots with the "trash blanket" (leaves and other residues from harvesting). This method is notoriously difficult and time consuming and results in increased harvest costs. The method does, however, have its advantages such as the preservation of soil moisture, suppressed weed growth, improved pest control, and increased soil nutrient value due to the organic matter, which also reduces field damage under wet conditions.

Besides the short-term financial benefit of the preharvest burns, there are adverse impacts on the environment that should be considered such as the emission of greenhouse gases, particulate matter, and semivolatile organic compounds (SVOCs) into the atmosphere. The smoke produced from these burning events is also hazardous to nearby road users, and the ash from the burns may end up in sensitive areas such as beaches, residential areas, and schools. The harvest season of sugar cane lasts between 5 to 6 months, and during this time a significant number of atmospheric pollutants are emitted into the atmosphere that may have a negative impact on human and environmental health (SASA, 2012).

Among the organic pollutants emitted are polycyclic aromatic hydrocarbons (PAHs), which are ubiquitous in the environment and contain two or more fused benzene rings in varying arrangements. They are formed through a pyrolytic process during incomplete combustion of organic materials and in emerging economies, such as South Africa, prominent sources include biomass burning, vehicular emissions, and indoor wood burning for heating and cooking (Dat & Chang, 2017; Forbes & Rohwer, 2009). Due to their well-researched potential carcinogenicity, teratogenicity, and genotoxicity, the US Environmental Protection Agency (USEPA) has identified 16 priority PAHs, and the World Health Organization (WHO) has added 17 additional PAHs, for a total of 33 PAHs under regulation by the WHO (Chen et al., 2017; Dat & Chang, 2017; Keith, 2015; Rengarajan et al., 2015).

Ambient PAH levels depend largely on the sources of PAHs nearby, with PAH concentrations generally being higher in industrial, urban, or residential areas compared with remote or rural sites, with PAH concentrations measured in ambient air worldwide therefore varying from less than 50 pg m^{-3} to more than 1.7 μg m^{-3} (Dat & Chang, 2017). Furthermore, ambient PAH concentrations also depend on the prevailing metrological conditions such as wind direction, wind speed, relative humidity, and temperature. Seasonal variation in PAH concentrations validate the importance of these meteorological parameters, although sources also vary seasonally with respect to emission rates, with higher PAH concentrations being reported in winter (Dat & Chang, 2017). A recent Iranian study found that summed PAH concentrations were 0.008–59.46 (mean: 11.61) ng m^{-3} and 0.05–40.83 (mean: 10.22) ng m^{-3} for the cold and warm seasons, respectively (Nadali et al., 2021).

These seasonal PAH variations can be explained by reduced radiation during winter resulting in a reduction of photo-, thermo-, and chemical oxidations in the atmosphere. In addition, a thinner planetary boundary layer and frequent thermal inversions may trap pollutants in the lower troposphere and prevent their dispersion, resulting in higher winter values, whereas in summer seasons, lower PAH concentrations can be partially attributed to increasing PAH volatilization from particle to gas phase and better dilution and dispersion of atmospheric PAHs. Wind speed and relative humidity were also found to be significant predictors for both light and heavy PAHs because higher wind speeds may reduce PAH levels by increasing dilution and dispersion of air masses, and an inverse correlation between PAHs and wind speed was also observed by other authors (Sharma et al., 2007; Tan et al., 2006, 2011).

The contribution of various parameters such as temperature, relative humidity, rainfall, atmospheric pressure, and wind speed on total and individual PAH concentrations was investigated by Amarillo and Carreras (2016). The authors found that temperature was the meteorological parameter that affected the total and individual PAH concentrations the most, with a stronger influence on light than heavy PAHs because they are more easily partitioned into the vapor phase (Amarillo & Carreras, 2016). Masih et al. (2012) found that PAH concentrations decreased with an increase in temperature and wind speed, whereas Elorduy et al. (2016) reported a relatively low correlation between PAH concentration and humidity and concluded that temperature and wind speed might be the major meteorological factors affecting the concentration of atmospheric PAHs.

To add to the complexity of PAH emissions, they undergo various transformations in the atmosphere depending on whether the PAH is in the gas phase or if it is associated with particles, which is why it is vital that the concentration of PAHs in both phases be determined, to accurately assess the health and environmental risks they pose. The partitioning of PAHs between the gas and particle phase depends on a few aspects including the volatility of the compound, ambient temperature, and the atmospheric concentration of particles. Smaller PAHs (two- to four-ring) tend to be more present in the gas phase, and the larger PAHs (more than four rings) in the particulate phase (Godoi et al., 2004; Vione et al., 2004). Meteorological parameters such as relative humidity, precipitation, temperature and the concentration of ambient dust or particulate matter also influence the partitioning (Kural et al., 2018).

Quantification of PAHs from two municipalities in Mexico with different climatic conditions, during sugar cane harvest seasons showed that the most abundant particulate PAHs were the larger five- to six-ring PAHs, namely, indeno[*1,2,3-cd*]pyrene, benzo[*b*]fluoranthene, benzo[*a*]pyrene, and dibenzo[*a,h*]anthracene. The ∑PAHs associated with particulate matter (PM)10 and PM2.5 ranged from 4.34 to 8.40 and 3.70 to 5.80 ng m^{-3}, respectively. That study is unique in that it accounts for the sugar cane harvest as well as the milling processes that emit pollutants into the atmosphere (Mugica-Alvarez et al., 2015). In a Brazilian study by de Andrade et al. (2010), the average ambient concentrations of total PAHs associated with atmospheric particulate matter were found to be 22.90 ng m^{-3} during August 2002 and September 2003 (falling within the annual sugar cane burn season), which was significantly higher than 2.35 ng m^{-3} for the non-burn period, indicating that the

burning of sugar cane was the main contributor to the high levels of PAHs in Araraquara, Brazil. In another Brazilian study, soot samples were collected in the sugar cane fields after burning and thereafter extracted and analyzed by gas chromatography–mass spectrometry (GC–MS) to reveal that 31 PAHs were detected; the authors concluded that their findings should serve as additional caution to workers and the general population to avoid exposure to the fly soot (Zamperlini, Silva, & Vilegas, 1997).

Due to the rise in awareness of the potential impacts of biomass burning and associated pollutants, emission factors were calculated with the aim of making source-specific emission estimates for area-wide inventories. Hall et al. (2012) reported total PAH emission factors of 7.13 ± 0.94 and 8.18 ± 3.26 mg kg^{-1} for dry leaf and whole sugar cane stalk burning, respectively, for preharvest burning in Florida. The most predominant PAH was found to be the lower molecular weight naphthalene. Ultrafine PM (PM0.1 μm) and particle-bound PAH emission factors were also determined in a study by Samae et al. in 2021, in which combustion of various biomasses, including sugar cane bagasse and sugar cane leaves, was carried out in a tube furnace; the emitted PM was collected using a nanosampler with size segregator. Chrysene, benzo[*b*]fluoranthene and benzo[*k*]fluoranthene were the dominant PAHs found on PM < 0.1 μm in size, with the general finding that four- to six-ring PAH concentrations were the highest in PM samples < 0.1 μm (Mugica-Álvarez et al., 2018; Samae et al., 2021). Sevimoglu and Rogge (2016) collected 24-h size-segregated samples for 12 months in Florida (USA), during sugar cane burning seasons using a high-volume sampler with a PM10 selective inlet. The authors concluded that 55%–70% of the total PAHs were associated with particles having diameters smaller than 0.49 μm. The PAH levels during the burn season ranged from 3.00 to 7.36 ng m^{-3} in rural and urban regions, respectively, which were 15 times higher than during the growing season (Sevimoglu & Rogge, 2016).

Numerous other studies found in the literature pertaining to sugar cane burning have primarily paid attention to the toxicity of PAHs associated with PM, but it has been found that many anthropogenically sourced PAHs are emitted predominantly in the gas phase (Geldenhuys et al., 2015). The difficulty around the various methods used to sample semivolatile PAHs is that they require larger sampling volumes and extended sampling times to accurately quantify trace levels in ambient air, after which complicated and time consuming pretreatment and concentration procedures are employed to prepare the sample for instrumental analysis (Godoi et al., 2004; Pandey et al., 2011; Poster et al., 2006). These sampling strategies run the risk of analyte breakthrough and blow-off, and vital PAH partitioning information is lost, not to mention the introduction of unwanted sampling artifacts. Thus it is vital to overcome these sampling bottlenecks and include a simplified sampling method that is able to adopt low flow rates, short sampling intervals, and simultaneous sampling of gas and particle phase PAHs in a manner in which their partitioning is unaffected by sampling conditions.

We have characterized and quantified both gas and particulate PAH emissions from preharvest sugar cane burning events and evaluated the influence on such emissions of weather and crop conditions. To the best of our knowledge, ours is the first study to fully characterize PAHs in both phases in emissions from sugar cane burning in South Africa and also the first study to consider the influence of crop variety on the resultant PAH emissions. We collected PAHs in both gas and particle phases simultaneously using small portable denuder sampling devices that minimized sampling artifacts; each denuder component could be directly thermally desorbed, which avoids time-consuming and environmentally unfriendly sample preparation procedures. This type of sampling device has been effectively used and validated in previous studies (Forbes, 2015; Geldenhuys et al., 2015; Kohlmeier et al., 2017; Munyeza et al., 2019). Our study, and others like it, are important for establishing best practice in sugar cane harvesting and related air quality monitoring, thus helping to enhance the environmental benefits of the sugar cane industry and its sustainability.

MATERIALS AND METHODS

Sampling sites

Samples were taken at five different sites situated in the province of Kwa-Zulu Natal in South Africa (Figure 1A). The two sampling regions included the Kwa-Zulu Natal North Coast, which is a coastal region at low altitude with a warm and temperate climate, whereas the Kwa-Zulu Natal Midlands is situated more inland, at higher altitudes (>800 m above sea level), and has a more moderate maritime climate with typical warm rather than hot summers and cool to cold winters. During the month of August when sampling took place, the coastal areas experienced lower humidity of 50%–60% and less rainfall than the annual average, whereas the Midlands also experienced the lowest humidity (45.6% average relative humidity) and precipitation in August, but this was accompanied by maximum sustained winds (Climate-Data.org, nd).

Each of the farms differed in terms of size and location, as well as the age, height, and sugar cane crop variety. A total of five burn events were sampled, as summarized in Table 1. Meteorological data were extracted from fixed weather stations operating at each site and were also collected on-site using a hand-held Kestrel 4500 Pocket Weather Tracker (KestrelMeters). The burns were started along the downwind edge of the field, against wind, to reduce the speed of the burn and optimizse the control thereof.

At each burn event, polydimethylsiloxane (PDMS) denuders and aethalometer samples were taken before and during the burn at a stationery point at a distance of approximately 16 m from the edge of the sugar cane field (Figure 1B). In addition, three aethalometer samplers were used as personal samplers worn by the researchers while walking around the field during the burns, which would result in measurements comparable to a farm worker's worst-case personal exposure, because the workers generally remain upwind to stay clear of the smoke.

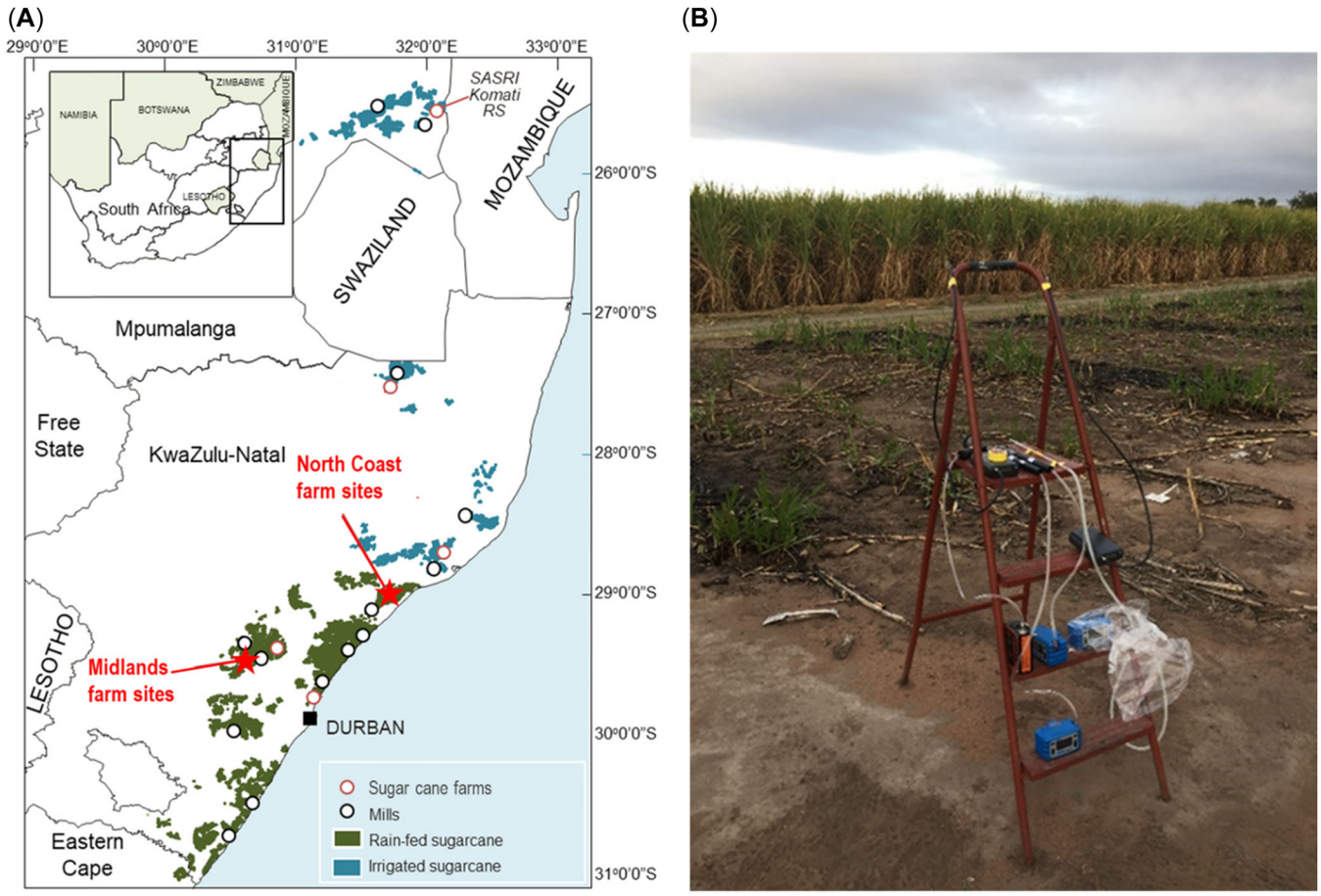

FIGURE 1: (**A**) Sampling locations in the South Africa sugar belt in Kwa-Zulu Natal Province in South Africa (adapted from SASA, 2022). (**B**) The sampling setup during burning events.

Sampling

PDMS denuder sampling devices. The PAH samples were collected with Gilair Plus personal sampling pumps (Sensidyne) attached to the denuder devices via Tygon® thermoplastic tubing. The GilAir pumps were operated at a low flow rate of 0.5 L min^{-1} to prevent breakthrough of the more volatile PAHs from the denuder traps. The denuder sampler consisted of two multichannel silicone rubber traps (each trap: 178-mm-long glass tube, 4.0-mm i.d., 6.0-mm o.d.) each containing 22 parallel PDMS tubes (55 mm long, 0.3-mm i.d., 0.6-mm o.d.) separated by a 6-mm-diameter quartz fiber filter (QFF), held in position by a Teflon connector. This configuration allows for both gas and particulate phase sampling and has been validated in numerous studies (Forbes, 2015; Forbes et al., 2012; Forbes & Rohwer, 2009; Kohlmeier et al., 2017; Munyeza et al., 2019). The gas phase SVOCs were trapped by the first (primary) trap because the PDMS served as a solvent for these compounds; the particles were then trapped downstream on the QFF. The postfilter trap (secondary trap) served to sample any blow-off. Figure 2 illustrates the sampling setup whereby each sample taken resulted in three individual samples, namely, the primary trap, the filter, and the secondary trap samples. A total of 14 samples (denuders) and two field blank samples were taken, as summarized in Table 1.

Samples were taken before and after burn events at five different sites. The upwind sample was taken prior to the burn event and represented background "clean air" that was not affected by the specific biomass burning event itself, but may have been affected by other burns in the vicinity or previous burns in the area, as well as non-biomass combustion sources of PAHs. The downwind sample was taken during the burn event in the plume of the smoke generated from the fire. This sample was taken for 10 min and thus provides a snapshot of the air quality at that specific time and position.

Field blank samples were taken at the burn events and treated in the same manner as other samples but were not connected to the sampling pump. These samples were used to determine any contamination introduced during handling and transport of samplers prior to analysis. The PAH concentrations detected on the field blanks were subtracted from all upwind and downwind samples to correct for any handling and storage contamination. The upwind samples were subtracted from the downwind samples when PAH emissions and profiles resulting from the burn event alone were considered; in the present study the upwind samples were treated as background pre-burn conditions.

TABLE 1: Sample site (farm), location of crop information, and meteorological sampling details for each sampled burn event

Parameter	Kearsney	Gingindlovu	Glenside 23E	Glenside 57	Glenside 58
Burn event	1	2	3	4	5
Location	Kwa-Zulu Natal North Coast	Kwa-Zulu Natal North Coast	Kwa-Zulu Natal Midlands	Kwa-Zulu Natal Midlands	Kwa-Zulu Natal Midlands
Altitude (m)	170	60	942	888	882
GPS coordinates	29° 17′ 42.7″S 31° 16′ 13.1″E	29° 01′ 41.1″S 31° 36′ 31.9″E	29° 20′ 56.7″S 30° 46′ 05.8″E	29° 21′ 09.4″S 30° 46′ 19.3″E	29° 21′ 17.4″S 30° 46′ 16.5″E
Crop variety	N58: The crop residue is abundant and adhering very strongly	Mixed	N42: Light canopy. The older leaf sheaths or trash virtually cover and enclose the whole stalk	N57: Excellent canopy with fairly erect leaves (some bend near tip) of medium width. The trash is clingy and abundant	N58: The crop residue is abundant and adhering very strongly
Crop age (mo)	14	18	20	Unknown	20
Burn type and observations	Fast, hot burn, lit upwind	Slow burn	Hot burn due to dry conditions. More black particulates observed due to dryness and compact dense growth of cane (lots of leaf material). Petrol/diesel mix used to light.	Cooler burn due to early morning dew and still conditions. Plume dispersed fast with little residual smoke. Burn was fast and contained	Slow burn
Weather conditions	Cloudy, cool, gusty winds	Clear sky, gusty winds	Cloudy, cold, windy	Partly cloudy, no wind	Cloudy, cool, gusty winds
Burn start–end time	7:00–7:45	15:07–16:00	15:37–16:30	7:20–8:00	14:48–15:32
Air velocity at sampling point (m s^{-1})	1.6	4.4	2.4	0.1	3.5
Wind direction	W	SSW	SSE	W	S
Barometric pressure (hPa)	992.8	1012.5	904.7	910.7	911.6
Temperature (dry bulb [DB] and wet bulb [WB] °C)	16.9 (DB) 16.2 (WB)	21.2 (DB) 16.8 (WB)	14.6 (DB) 14.1 (WB)	12.4 (DB) 10.5 (WB)	15.2 (DB) 10.9 (WB)
Humidity (%)	66.5	59.2	54.1	94.3	84.5
Solar radiation (W m^{-2})	29.4	370.8	208.0	38.0	165.7
No. of stationary samples taken					
PDMS denuders	2	4	2	2	4
Aethalometer	2	2	2	2	2
No. of personal samples taken					
Aethalometer	3	3	3	3	3

PDMS = polydimethylsiloxane.

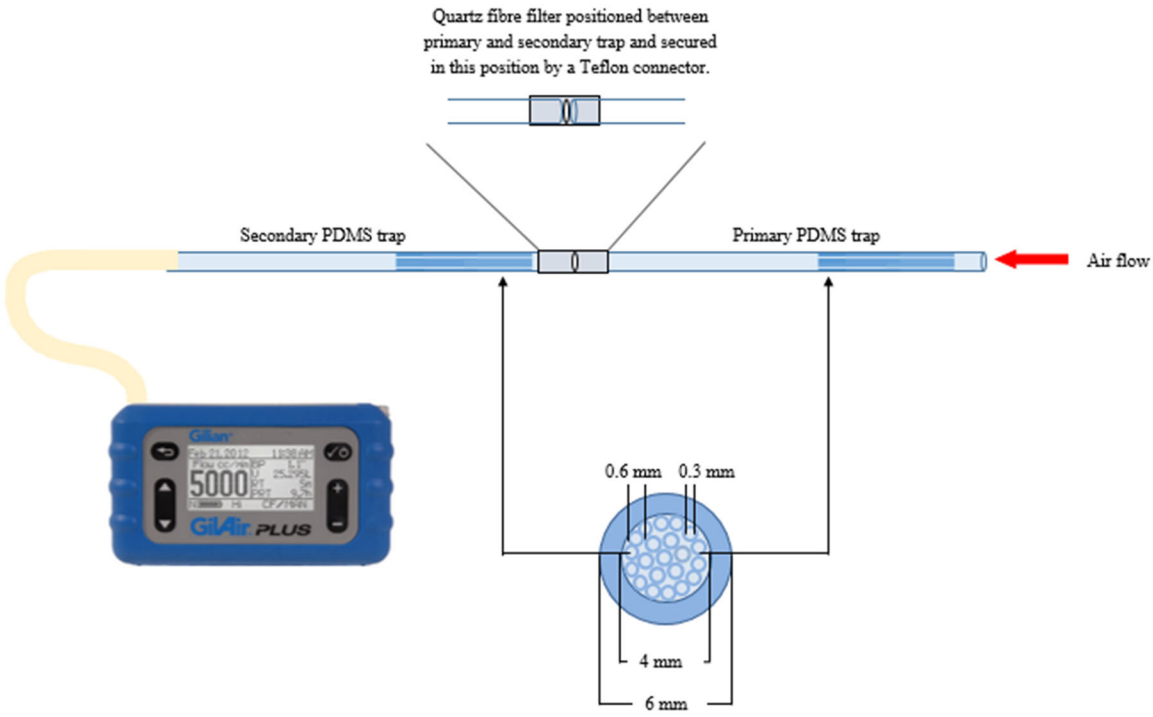

FIGURE 2: Schematic of the denuder sampling device consisting of a primary trap, filter, and secondary trap for simultaneous gas and particulate sampling (Geldenhuys et al., 2015). PDMS, polydimethylsiloxane.

Black carbon monitoring with portable aethalometers.

Portable aethalometers (microAeth®, MA 200 series, AethLabs) were employed during all sampling events. Aethalometers are portable instruments, equipped with an internal pump, that allow for online monitoring of carbonaceous aerosol particles by measurement of their light attenuation. The aerosol particles were continuously deposited on a polytetrafluoroethylene filter tape and were monitored at five different wavelengths (375, 470, 528, 625, and 880 nm) ranging from ultraviolet to near infrared. The aethalometers were used as personal and stationary samplers as discussed in the *Sampling sites* section.

Analytical techniques

Offline analysis of each individual denuder component was performed using a LECO Pegasus four-dimensional instrument consisting of a comprehensive two-dimensional GC coupled to a time-of-flight mass spectrometer (GCxGC–TOF–MS). The instrument was equipped with an Agilent Technologies 7890 GC, a quad jet dual-stage modulator, and a secondary oven. Data acquisition and processing were executed by ChromaTOF Ver 4.0 and ChromaTOF Tile software (LECO). A Gerstel 3 thermal desorption system (TDS) was employed for sample introduction whereby the PDMS traps were directly thermally desorbed, and the filter samples were inserted into the heating zone of an empty precleaned glass tube for desorption. Synthetic air was used for the hot jets, and liquid nitrogen was used to cool nitrogen gas for the cold jets with an AMI model 186 liquid level controller to maintain sufficient levels. The GC column set consisted of a Restek Rxi-1MS nonpolar phase 100% dimethyl polysiloxane (30 m, 0.25 mm i.d., 0.25 µm df) as the first dimension (1D) and an Rxi-17Sil MS, midpolar 50% phenyl 50%-dimethyl polysiloxane (0.79 m, 0.25 mm i.d., 0.25 µm df) as the second dimension (2D). Thermal desorption occurred from 30 to 280 °C at a rate of 60 °C min^{-1} and was held for 5 min during which the analytes were cryogenically focused via a cooled injection system at −50 °C using liquid nitrogen. The temperature was ramped at 12°C s^{-1} to 280 °C, and the inlet purge time was 3 min. The desorption flow rate was 100 ml min^{-1}, and the TDS transfer line was set at 300 °C. The primary oven was ramped at 5 °C min^{-1} from 40 to 315 °C, which was held for 15 min. The secondary oven was offset by 5 °C, and the modulator temperature was offset by 30 °C. The modulation period was 3 s with a hot pulse time of 1 s. The MS transfer line temperature was set to 280 °C, and mass acquisition ranged from 50 to 500 Da at 100 spectra s^{-1}. The electron energy was 70 eV, and the ion source temperature was 200 °C.

Matrix-matched calibration standards

Calibration was performed using a certified standard PAH mix solution (Supelco), containing 15 priority PAHs. The nominal concentration of each compound in the mixture dissolved in methylene chloride was 2000 µg ml^{-1}. The names and abbreviations of the PAHs included are given in Table 2. A stock solution at a concentration of 100 µg ml^{-1} was prepared in toluene, and working solutions were prepared by appropriate dilutions of the stock solutions in n-hexane before use. All solvents used for dilutions and cleaning procedures were of analytical grade (99% purity) including toluene, methanol, dichloromethane (DCM), and n-hexane (all from Sigma-Aldrich) and acetone (from Associated Chemical Enterprises). The deuterated internal standards

TABLE 2: Analytes investigated in the present study including 15 of the 16 US Environmental Protection Agency priority polycyclic aromatic hydrocarbons (PAHs) and their corresponding abbreviations, molar masses, and boiling points

Formula	PAH name	Abbreviation	Molar mass (g mol^{-1})	Boiling point (°C)
$C_{10}H_8$	Naphthalene	Nap	128	218
$C_{11}H_{10}$	1-Methyl naphthalene	Nap 1 M	142	240
$C_{12}H_8$	Acenaphthylene	Acy	152	265
$C_{12}H_{10}$	Acenaphthene	Ace	154	278
$C_{13}H_{10}$	Fluorene	Flu	166	295
$C_{14}H_{10}$	Phenanthrene	Phe	178	339
$C_{14}H_{10}$	Anthracene	Ant	178	340
$C_{16}H_{10}$	Fluoranthene	FluAn	202	375
$C_{16}H_{10}$	Pyrene	Pyr	202	360
$C_{18}H_{12}$	Benz[*a*]anthracene	BaA	228	435
$C_{18}H_{12}$	Chrysene	Chy	228	448
$C_{20}H_{12}$	Benzo[*b*] fluoranthene	BbF	252	481
$C_{20}H_{12}$	Benzo[*a*]pyrene	BaP	252	495
$C_{22}H_{12}$	Benzo[*g,h,i*] perylene	BghiP	276	536
$C_{22}H_{12}$	Indeno[*1,2,3-cd*] pyrene	I123P	276	536
$C_{22}H_{14}$	Dibenz[*a,h*] anthracene	DbahA	278	524

Data from PubChem, 2021.

(I_{Std}) d_8-naphthalene, d_{10}-phenanthrene, d_{10}-pyrene, and d_{12}-chrysene were obtained from Isotec (Sigma-Aldrich) and were used in all standards and samples.

Gas phase PAHs quantification was achieved by analyzing individual conditioned PDMS traps that were spiked with 1 µl of the following concentrations of mixed PAH standard in toluene: 0.1, 0.5, 1.0, 2.0, 5.0, 10.0, and 20.0 ng µl^{-1}. Similarly, to quantify particle bound PAHs, precleaned 6-mm QFF punches were spiked with 1 µl of 0.1, 0.5, 1.0, 2.0, 5.0, and 10 ng µl^{-1} mixed PAH standards in toluene.

Quality assurance

The PDMS traps were conditioned prior to use at 280 °C for 16 h under hydrogen (99.999% or more purity; AFROX) with a gas flow of 100 ml min^{-1} using a Gerstel TC 2 Tube Conditioner. Quartz fiber filter punches were rinsed twice with DCM and methanol after which they were dried in an oven at 200 °C for 2 h and stored in an amber vial in a desiccator prior to use. Immediately after sampling, the filters were stored in amber vials, and the traps were sealed with end caps. Each denuder component was individually wrapped in sterilized aluminum foil and placed in separate Ziploc bags in a cooler box containing ice packs on site. The samples were then were placed in a freezer at −18 °C between the time of collection and analysis.

Calibration was performed in duplicate, and 1 µl of an I_{Std} mixture, containing d_8-naphthalene, d_{10}-phenanthrene, d_{10}-pyrene, and d_{12}-chrysene (1 ng µl^{-1}) was spiked onto all samples and standards prior to analysis to correct for any instrument variability or matrix effects; calibration curves were derived from the area ratio of target analyte: I_{Std}. Procedural blanks were analyzed in conjunction with the samples to ensure no carryover. Linear regression analyses were performed using the Data Analysis Toolkit in Excel, and correlation of determination values of more than 0.90 were used as a statistical measure to indicate a good linear fit and validate the analyte method. The limit of detection (LOD) of each target compound was calculated as 3 times the signal-to-noise (S/N) peak-to-peak ratio and the limit of quantitation (LOQ) as 10 times the S/N ratio using the lowest concentration calibration standard. The LOD and LOQ values for PDMS trap and QFF samples are presented in Table 3. The LOD values ranged from 0.06 to 9.12 ng m^{-3} for the PDMS traps and 0.04 to 6.41 ng m^{-3} for the QFF samples.

TABLE 3: Limits of detection and limits of quantification for individual polycyclic aromatic hydrocarbons detected in polydimethylsiloxane trap and quartz fiber filter samples (ng m^{-3})

	PDMS trap		QFF	
PAH	LOD	LOQ	LOD	LOQ
Nap	0.06	0.19	0.04	0.15
Nap 1 M	1.15	3.82	0.20	0.68
Acy	1.98	6.61	0.47	1.57
Acey	0.89	2.97	0.86	2.88
Flu	1.17	3.89	2.08	6.94
Phe	6.58	21.92	4.32	14.39
Ant	4.15	13.84	1.18	3.92
FluAn	9.12	30.39	6.41	21.38
Pyr	8.56	28.55	5.46	18.19

LOD = limit of detection; LOQ = limit of quantitation; PAH = polycyclic aromatic hydrocarbon; QFF = quartz fiber filter; PDMS = polydimethylsiloxane. See Table 2 for other abbreviations.

Statistical evaluation

Statistical evaluation, including principal component analysis (PCA), was performed using XLSTAT (Addinsoft) software and ChromaTOF Tile (LECO). A p value of 0.05 was used for data comparison among the primary trap, the filter, and the secondary trap, and F ratios were evaluated for the significant compounds (F ratio greater than 100). Supporting Information, Table S2, details the method parameters for the PCA analysis.

RESULTS AND DISCUSSION

The type of burn, speed of burn, and prevailing weather and crop conditions all had an influence on the resultant PAH concentration. These conditions and any significant observations are detailed in Table 1. Field blank samples were taken at burn events at which only traces of naphthalene and 1-methyl naphthalene were detected and were corrected for in the samples; the concentrations of PAHs detected on the field blank samples are reported in the Supporting Information, Table S1.

Total PAH emissions

Figure 3 depicts the ΣPAHs from all five burn events. It is immediately evident that downwind PAH concentrations were

significantly higher than the upwind samples, and it can be concluded that the preharvest burning of sugar cane biomass is a major source of PAHs in the atmosphere during a burn event. Likewise, in another similar study in Florida (USA), it was concluded that the sugar cane harvesting season resulted in 15x higher PAH concentrations than during the growing season, indicating a substantially higher exposure of the population to PAHs due to the burning events (Sevimoglu & Rogge, 2016). More recently, the same authors also positively correlated the ambient concentrations of PAHs with the biomass combustion markers levoglucosan and potassium during burn events (Sevimoğlu & Rogge, 2019).

The sources of the background PAHs in the upwind samples could be attributed to the burns that were underway or had taken place in the area or from diesel exhaust emissions from vehicles operating nearby including the water truck that is required to be present during burning events in case of emergency or wildfire. Cigarette smoke from the farm workers was also documented as a potential source of PAHs in the ambient air.

In the present study, the total PAHs in the primary trap samples for all the burn events (adding up to 17.2 $\mu g\,m^{-3}$) accounted for over 90% of total PAHs detected in the samples, signifying that the majority of PAHs were in the gas phase and that determination of PAHs associated with PM only would lead to a gross underestimation of potential environmental and human health impacts.

The majority of the samples showed the detection of both gas and particulate PAHs, which is consistent with denuder theory in which the primary PDMS trap sorbed gas phase analytes while particle-associated analytes passed through the trap and were collected on the downstream filter. Particle-bound analytes primarily remain particle bound on the filter, but should they blow off from the filter, they are trapped on the secondary trap. Blow-off is loss of particle phase analyte caused by the pressure gradient existing through the filter (Kumari & Lakhani, 2018) and disturbance of the gas particle equilibrium (Forbes & Rohwer, 2009). In the present study, the loss due to blow-off is expected to be minimal because of low sampling flow rates and sampling intervals. In addition, the low back pressure across the denuder sampling device throughout this sampling interval reduced the potential for such effects to occur.

The upwind samples at each site showed the detection of two-ring 1-methyl naphthalene in the range of less than LOQ to 0.10 $\mu g\,m^{-3}$. The background contribution of lighter PAHs from the secondary trap samples may be due to breakthrough of the most volatile PAHs from the primary trap, because the denuder devices are validated to have a breakthrough volume of 5 L for naphthalene at a sampling flow rate of 500 $ml\,min^{-1}$ (Forbes et al., 2012; Forbes & Rohwer, 2009). Our sampling volumes were slightly higher than this, with an average sampling volume of 5.20 ± 0.70 L, leading to the slight breakthrough of the two-ring PAHs. Another consideration is that these small PAHs can be transiently associated with particles and seeing that the two-ring PAHs are the most volatile, loss by volatilization from the filter may occur during sampling.

For the downwind samples, the temperatures at the sampling locations were higher than ambient temperatures, due to the burning event, and thus the breakthrough volumes would be slightly reduced because the higher temperatures reduce sorption capacity of analytes and hence reduce retention on the primary PDMS trap. Nonetheless, these PAHs would be subsequently trapped downstream on the secondary PDMS absorbent and no loss of analyte would result.

When looking at each burn event individually (Figure 4 and Supporting Information, Table S1) a distinct difference in

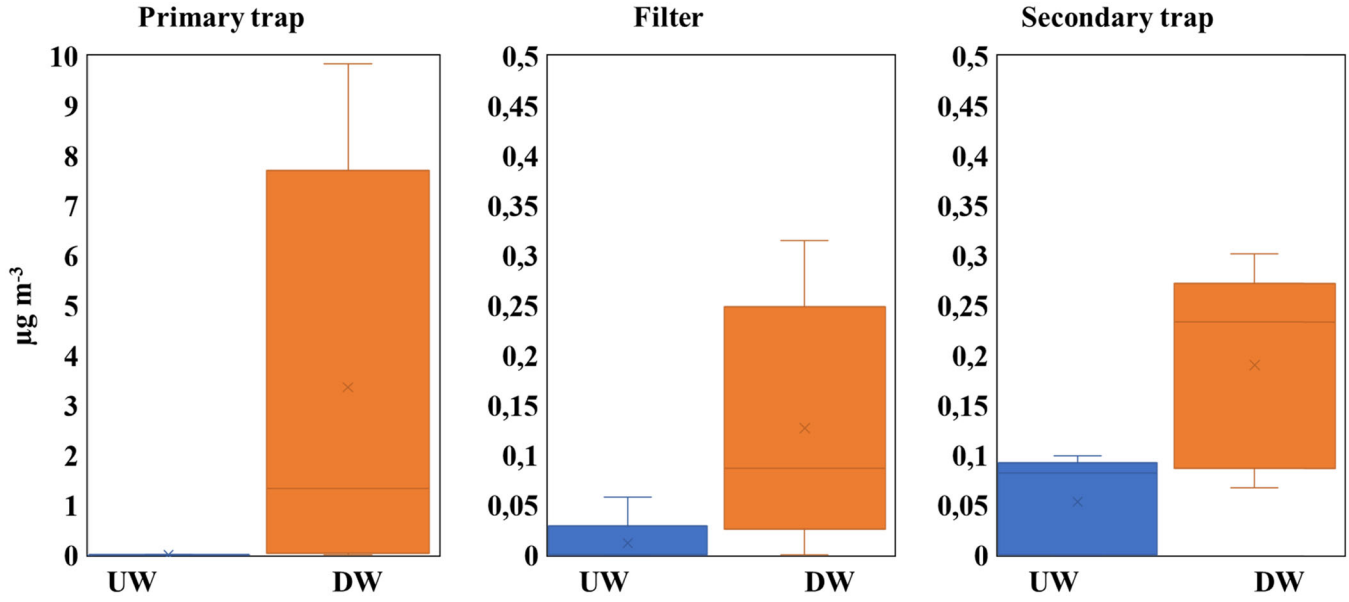

FIGURE 3: Box plot representing the sum of polycyclic aromatic hydrocarbons (PAHs) detected on the primary trap, filter, and secondary trap per burn event in upwind (UW) and downwind (DW) samples (total $n = 39$ for all plots with each plot representing $n = 5$ across the five burn events). The maximum and minimum values represent the extreme PAH concentrations found at burn events, with the area between the 25th and 75th percentiles representing the spread of PAH concentration between the other burn events.

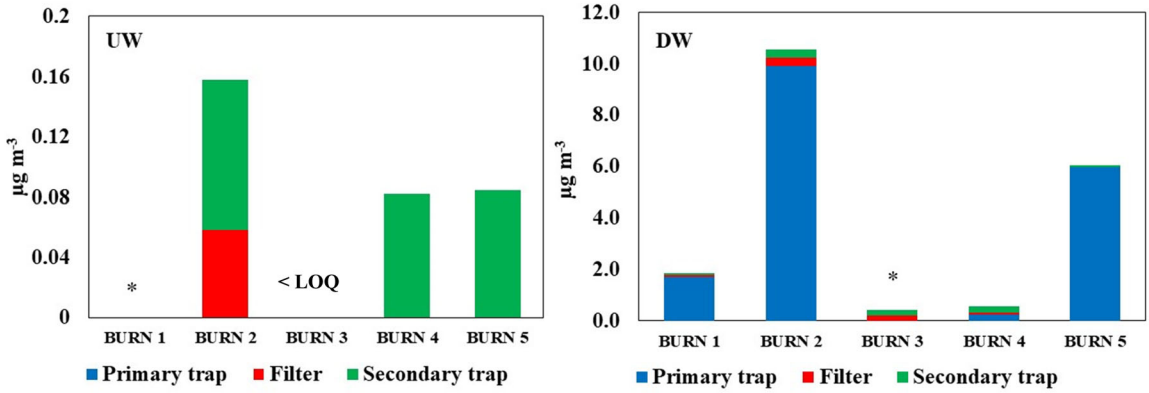

FIGURE 4: Upwind (UW; left) and downwind (DW; right) total polycyclic aromatic hydrocarbon (PAH) concentrations found on the primary trap, filter, and secondary trap of the denuder device per burn event (1–5) *Burn 1 upwind filter and secondary trap were in-field sample losses, and Burn 3 downwind primary trap was lost due to a power outage during instrumental analysis. LOQ = limit of quantitation.

concentration can be seen between each burn event that can be attributed to the prevailing weather conditions, variations in the crop variety (moisture and leaf matter), and the nature of the burn event. Figure 4 shows the variation in PAH concentration and PAH partitioning between burn events for both upwind and downwind samples. The variation emphasizes the effect that the prevailing weather, crop, and burn conditions have on the emissions. The upwind filter and secondary trap of Burn 1 fell off the sampling ladder onto the floor and were excluded from the sampling set due to possible contamination. The downwind primary trap of Burn 3 was not included due to technical complications during analysis. The lost samples were not included in subsequent calculations.

From Figure 4, it can be seen that Burn 2 had the highest total PAH concentrations in both upwind and downwind samples, with the highest portion being represented by the downwind gas phase PAHs, equating to 10.23 $\mu g\, m^{-3}$. Burn 2 was the only burn event that was done during clear sky conditions, and it was accompanied by gusty winds. The higher ambient temperature and lower humidity compared with other burn events would be more conducive toward gas phase partitioning, which is confirmed by the largest portion of PAHs being detected on the primary trap samples. The burn event was a slow burn due to the gusty winds, which resulted in a smoldering fire, and poorer combustion conditions, and thus more combustion-associated emissions during the sampling interval.

Burn 5 also showed a significantly high gas phase PAH concentration, and this burn event was the only other burn event that was documented as a slow burn. The N58 crop variety had erect leaves with a more bare stalk compared with other varieties, and it also is characterized by abundant crop residue (South African Sugarcane Research Institute, 2022) that is strongly adhered to the stalk, which can influence the burning efficiency and may introduce a temperature gradient through the crop, leading to zones of poorer combustion efficiency and resulting in elevated PAH emissions.

Burn 4 had the lowest ΣPAH emissions in the downwind samples. This marked reduction in emissions can be partly attributed to the fact that a very narrow portion of the sugar cane was lit to start the event, and this was when the sampling commenced; therefore the volume of sugar cane burnt was initially smaller, resulting in fewer emissions during the short sampling interval. The crop variety characterized by abundant trash significantly contributed to efficient and contained combustion, which was evident by the small amount of residual smoke produced. The still conditions, trashy crop variety, and high humidity are variables contributing toward lower PAH emissions because the burn was characterized by higher flames and a faster and more contained burn with the least amount of residual smoke produced. As a result, Burn 4 can be an indicator of more favorable preharvest burn conditions not only for reduced PAH emissions but also for better control of the fire.

Although each burn event was recorded in as much detail as possible, it must be noted that there are certain limitations for direct comparability of events. Due to the different meteorological conditions, field orientations, field shape, crop size, and age, it was difficult to standardize the burns. It was not possible to get close to the field during the burn, for safety reasons, but it would be useful to be able to view and thus compare the burn events in real time. This may be possible with drone technology for safe and accurate comparison of real-life burning campaigns.

PAH Profiles

The individual gas and particle phase PAH fingerprints are presented in Figure 5 for each burn event. These concentrations are purely as a result of the burn event, because the PAHs detected in the upwind samples were considered as background concentrations and were thus corrected for in each downwind sample by subtracting the upwind PAH concentration from the corresponding downwind PAH concentration.

The fingerprints per burn event were similar in that the majority of the emissions were found to be in the gas phase with naphthalene being the most abundant PAH in each primary trap sample except for Burn 4, whereas the sample loss in Burn 3 cannot be commented on. However, the similarities end there: the concentration and range of individual PAHs differed

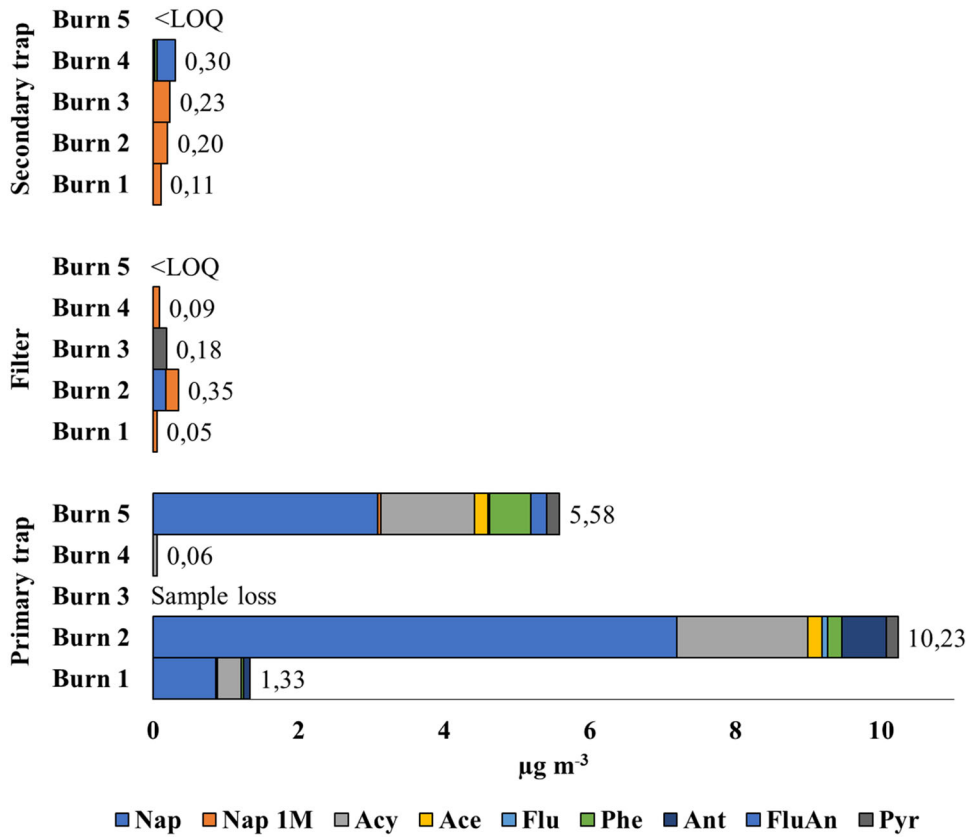

FIGURE 5: Individual polycyclic aromatic hydrocarbon (PAH) concentrations detected during each burn event on the primary trap, filter, and secondary trap of the denuder sampling device. LOQ = limit of quantitation. For other abbreviations, see Table 2.

significantly between each burn event. The concentration as well as number of PAHs also differed markedly between the primary trap and filter samples, indicating the complexity of the partitioning of PAHs with prevailing weather and burn conditions. The lower molecular weight PAHs such as naphthalene and 1-methyl naphthalene that were detected on the filter samples, which are normally partitioned in the gas phase, were likely in a condensed form due to the humidity before or during sampling. Kural et al. (2018) investigated the relationship between PAH concentrations and meteorological conditions in Istanbul, Turkey and reported that due to precipitation, high relative humidity, and high dust concentration, naphthalene was found in the condensed phase associated with particles. This complexity would be expected to increase even more with time due to additional atmospheric aging processes and reactions that occur resulting in the formation of secondary organic aerosols and harmful oxygenated and nitrated PAH derivatives (Keyte et al., 2016; Vione et al., 2004).

From Figure 5, it can be seen that the primary trap samples had the highest concentrations of PAHs, with Burn 2 and Burn 5 having the highest total PAH concentrations, of 10.23 and 5.58 µg m^{-3} respectively. The numbers of PAHs detected were also the most during these two burn events, ranging from two-ring naphthalene to four-ring pyrene. As discussed in the *Total PAH emissions* section, Burns 2 and 5 were conducive to higher incomplete combustion emissions based on the conditions of the burn, the crop variety, and meteorological parameters that consequently resulted in the formation of more PAHs including the higher molecular weight pyrene and fluoranthene. The slow burns associated with these two events produced more of a smolder than a high flame burn, which would result in incomplete combustion and overall lower temperature burns; they are also accompanied by higher amounts of PM, which act as nuclei for PAH particle associations. The overall gas-to-particle partitioning for these burn events favored the gas phase, which is influenced largely by the ambient temperature, relative humidity, and physical properties of the PAH.

The lowest total PAH concentrations of 0.06, 0.09, and 0.30 µg m^{-3} for the primary trap, filter, and secondary trap, respectively, are associated with Burn 4 (Figure 5). The lower total PAH emissions in this burn event can be mainly attributed to the fast and contained burn with more complete combustion. This burn event reflects the lowest number of PAHs in the gas phase, with 1-methyl naphthalene and acenaphthylene being the only PAHs detected on the primary trap. Interestingly, the secondary trap sample for Burn 4 showed the largest range of PAHs compared with the other secondary trap samples, with the detection of 1-methyl naphthalene, phenanthrene, and fluoranthene. The heavier PAHs have larger breakthrough volumes than naphthalene, so it is not likely due to breakthrough, and blow-off is expected to be minimal due to the sampling methodology; thus the presence of these PAHs on the secondary trap may be attributed to transient particle association. This can be explained by the substantially higher

humidity and lower ambient temperatures during Burn 4 compared with other burn events, which favored particle phase association.

The findings from our study were consistent with what was reported in a study by Li et al. (2016); these authors found that atmospheric PAH emissions due to biomass burning were dominated by the light PAHs: naphthalene, phenanthrene, pyrene, fluorene, acenaphthylene, anthracene, and acenaphthene (Chen et al., 2017; Li et al., 2016).

The presence of the heavier PAHs such as benzo[*a*]pyrene, benzo[*b*]fluoranthene, benzo[*ghi*]perylene, dibenz[*a,h*]anthracene, and indeno[*1,2,3-cd*]pyrene was not detected in any of the samples, which can be attributed to limits below quantification as well as the small sample volumes and amount of PM collected, because these analytes are expected to be predominantly particle associated; however, heavier PAHs have been detected and quantified with this analytical method previously (Geldenhuys et al., 2015). Desorption of SVOCs from PM on filters was optimized and demonstrated with TD–GCxGC–MS analysis in various other studies (Dragan et al., 2020; Schnelle-Kreis, Sklorz, et al., 2005; Schnelle-Kreis, Welthagen, et al., 2005); in the present study, the LODs for PAHs on the QFF ranged from 0.04 to 6.41 ng m^{-3} with the heavier four- to six-ring PAHs having the higher LODs. The LODs for PAHs on the traps ranged from 0.06 to 9.12 ng m^{-3} (refer to Table 3). Heavier four- to six-ring PAHs were detected in low concentrations in PM in other studies, with Sevimoglu and Rogge (2016) finding that 55%–70% of the total particulate PAH mass was associated with particle diameters smaller than 0.49 μm. These authors reported total particulate PAH levels of 7.36 ng m^{-3} in rural regions and 3.00 ng m^{-3} in urban regions during the sugar cane harvest season (Sevimoglu & Rogge, 2016).

Determination of PAH toxic equivalence

The toxic equivalency factor (TEF) method is employed to evaluate structurally related compounds sharing a common mechanism of action (Delistraty, 1997). Toxicity of a specific PAH is often expressed relative to benzo[*a*]pyrene. The potential carcinogenicity of the PAH exposure is estimated based on the calculation of toxic equivalent quotient (TEQ), whereby benzo[*a*]pyrene-like toxicity or toxic equivalents are determined using the following equation:

$$TEQ = \sum(PAH_i \times TEF_i),$$

where PAH_i and TEF_i are the concentration and TEF, respectively, for individual PAHs.

The TEFs were proposed by Nisbet and Lagoy (1992) based on the toxicity and carcinogenic potential of individual PAHs relative to benzo[*a*]pyrene. Table 4 shows the TEQ values that were calculated based on the determined concentrations of the total (gas and particle) PAHs (μg m^{-3}).

The highest risk potential of exposure was associated with Burn 2, which resulted in the largest TEQ. There are currently no exposure limits for PAHs in many countries, including South Africa; however, it is vital to understand the toxic equivalence concentration levels and potential health risks of exposure to PAHs to ensure that suitable risk assessment and risk management plans can be implemented. Several regulatory agencies such as the US Occupational Safety and Health Administration, the US National Institute for Occupational Safety and Health, and the German Committee on Hazardous Substances have imposed regulatory limits for coal tar pitch volatiles (benzene-soluble fraction) including anthracene, benzo[*a*]pyrene, phenanthrene, chrysene, and pyrene of 0.20 mg m^{-3} (Breuer, 2010; Rezaei et al., 2015). Although the $\sum$benzo[*a*]pyrene$_{TEQ}$ for each burn event is well below the referenced regulatory limit for coal tar pitch volatiles, these findings suggest that at levels encountered in the air during the sugarcane burning season, exposure to individual and complex mixtures of PAHs may pose an increased health risk that varies between burn events. It should be noted that the risk estimates presented are not definitive but should rather be seen only as a crude estimation of potential cancer risk from the PAH inhalation.

Principal component analysis

Principal component analysis is a statistical technique employed to create uncorrelated variables in large data sets to successively maximize variance. This tool aids in increasing interpretability of data while minimizing loss of vital information. Figure 6 shows the loading and scores plot for total PAH concentrations.

The loading and scores plots are depicted for total PAH concentrations between the five burn events and how they

TABLE 4: Toxic equivalency factor values for polycyclic aromatic hydrocarbons (PAHs) and the calculated toxic equivalent quotient values for total gas and particle PAHs (μg m^{-3})

PAH	TEF	Burn 1	Burn 2	Burn 3	Burn 4	Burn 5
Nap	0.001	4.04E-04	6.00E-04	2.34E-04	3.59E-04	4.84E-04
Acy	0.001	3.18E-04	1.80E-03		5.65E-05	1.29E-03
Ace	0.001		2.02E-04			1.89E-04
Flu	0.001		7.58E-05			2.52E-05
Phe	0.001	4.00E-05	1.99E-04		1.83E-05	5.59E-04
Ant	0.01	8.56E-04	3.02E-03			
FluAn	0.001				1.22E-04	2.21E-04
Pyr	0.001		8.05E-05	1.82E-04		1.76E-04
	$\sum$ BaP_{TEQ}	1.62E-03	5.97E-03	4.16E-04	5.56E-04	2.94E-03

PAH = polycyclic aromatic hydrocarbon; TEF = toxic equivalency factor. For other abbreviations, see Table 2.

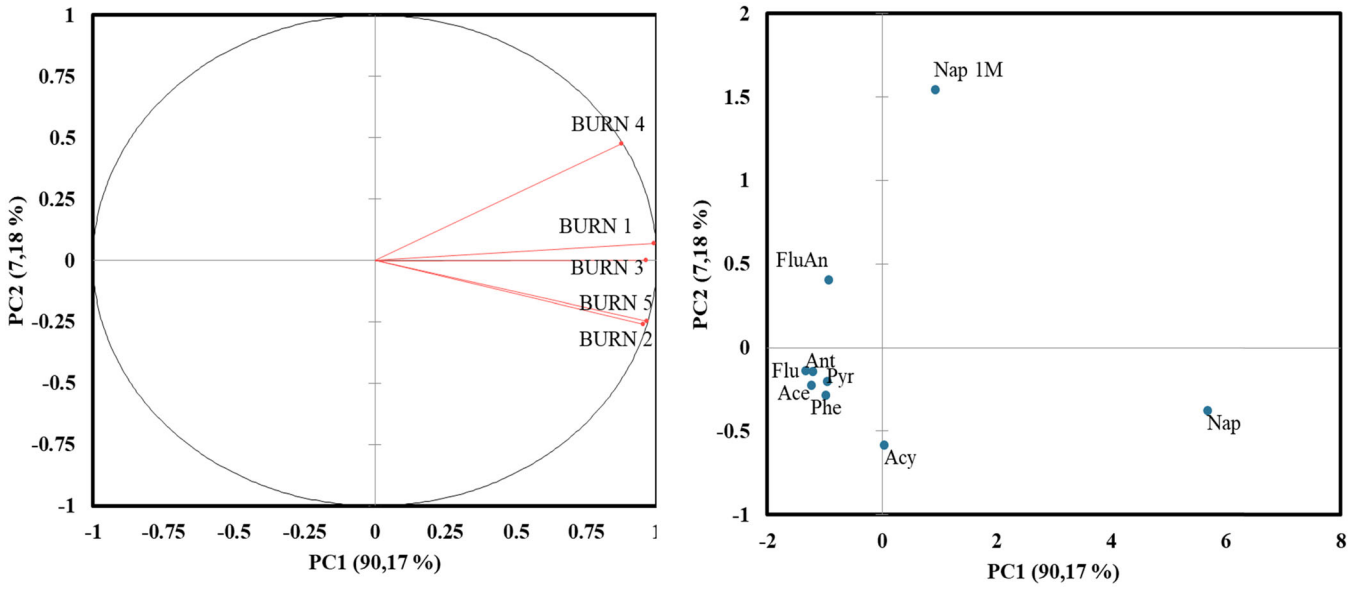

FIGURE 6: Loading plot (left) and scores plot (right) for total polycyclic aromatic hydrocarbon (PAH) concentrations (downwind [DW] gas + particle phase) between the different burn events. PC = principal component. For other abbreviations, see Table 2.

correlate to one another. The sum of components PC1 and PC2 accounted for 97.35% of variability from the initial data set. The first PC dimension represents 90.17% of the data, and the second PC dimension accounts for 7.18%. The angles between the vectors are all acute, indicating linked variables, and the vector lengths indicate the representativeness quality in the investigated PCA dimensions PC1 and PC2. which is very good. The loading plot validates previous discussion and shows the positive correlation between Burn 2 and Burn 5. Burn 4 shows the least correlation to the burn events in terms of PAH emissions. The scores plot relates individual PAHs to variables and to one another. The individual PAHs show that the lighter two- to three-ring PAHs, specifically naphthalene, 1-methyl naphthalene, and acenaphthylene, are the most significant contributors toward variance between burn sites. The variance between the burn events cannot only be attributed to the emissions and therefore Figure 7 also includes meteorological data to see the bigger picture and how numerous factors contribute to emissions.

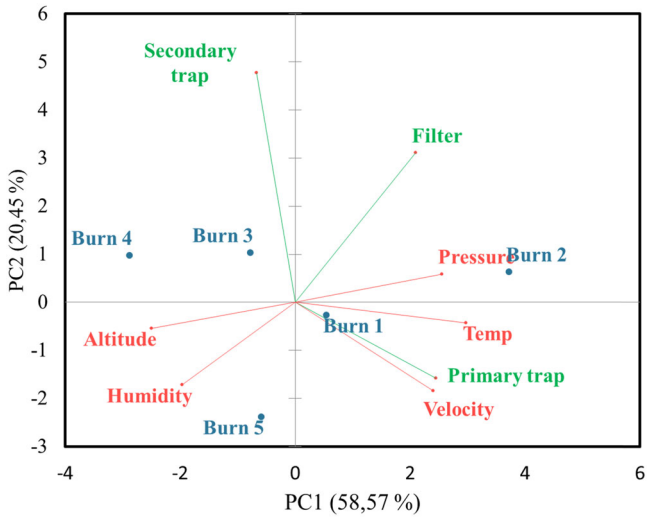

FIGURE 7: Biplot for sampling and meteorological variables relating to individual burn events. Total downwind (DW) polycyclic aromatic hydrocarbons (PAHs) on primary trap, filter, and secondary trap per burn event were used for the plot. PC = principal component.

To identify the influence that meteorological parameters may have had on the PAH concentrations at the different burn events, a second PCA was conducted. Although the sample set is limited, the analysis provides valuable preliminary information on the correlation of certain meteorological parameters with PAH concentration, as well as their impact on atmospheric partitioning. It is hypothesized that temperature will influence the partitioning, with higher temperatures favoring the gas phase, which was evident from the results (Figure 7) with a close correlation evident between temperature and the primary trap PAH concentration (which samples gas phase analytes). Humidity was expected to have a positive correlation to condensed particle phase PAH concentrations. The results showed some correlation with respect to PC1 between humidity and the secondary trap PAH concentration, which may relate to the repartitioning of particle phase analytes into the gas phase on re-equilibration during sampling. Higher wind speeds may result in lower total PAH concentrations due to dispersion and dilution effects, but in the case of biomass burning, wind speed also impacts combustion efficiencies and thereby PAH emissions. In Figure 7 a strong correlation between wind speed and primary trap PAH concentrations is evident.

The biplot showing the loading and scores plots is depicted for total PAH partitioning at each burn event as well as the inclusion of meteorological data as variables between the five sites (Figure 7). Axes PC1 and PC2 account for 79.02% of variability from the initial data set. The horizontal axis is the first PC dimension and represents 58.57% of the data, and the second

dimension accounts for 20.45%. The investigated variables are represented by the red vectors for the meteorological variables and green vectors for the primary trap, filter, and secondary trap samples. The vector lengths indicate the representativeness quality in the investigated PC dimensions PC1 and PC2. The acute angles between the filter and secondary trap samples indicate positively linked variables, which confirms the occurrences of transient particle association and the relationship among the primary trap, filter, and secondary trap samples and points to efficient denudation by the samplers. The biplot relating individual burn events to the discussed variables clearly indicates that there is significant variance between each burn event, with the PAH partitioning and atmospheric conditions being key contributors to the observed variance. The wind velocity was less of an influence than expected with Burn 2 and Burn 5 showing the highest gas phase PAH concentrations but also being the two events with the highest recorded wind speeds. The crop variety played more of an influential role in the number and type of PAHs emitted as well as the partitioning thereof. The expanded ChromaTOF Tile PCA score and loading plot with other significant chemical features associated with biomass burning within the primary trap, filter, and secondary trap can be found in the Supporting Information, Figure S1 and Table S3. The key chemical feature contributing to the variance from the filter samples was found to be phthalic anhydride, whereas 1,3-dioxolane and benzene 1-ethyl-4-methyl were the dominant features on the secondary traps. The loading plot was dominated by chemical features found on the primary traps, with benzaldehyde, tridecane, azulene, 1-methyl naphthalene, and furfural being the main markers influencing the principal components. Benzaldehyde is an intermediate in the atmospheric oxidation of aromatic compounds, and the presence of this compound, as well as other organic features identified, may contribute to the formation of ozone and secondary organic aerosols in the atmosphere air and further contribute to poor air quality.

Correlation of black carbon measurements to PAH concentrations

The portable aethalometers used during sampling provided measurements of equivalent black carbon originating from emitted biomass particles. Table 5 shows the mean equivalent black carbon concentrations, which were background-corrected using the upwind samples.

The highest values for black carbon were reported for Burn 2, with a mean value equating to 430.91 $\mu g\,m^{-3}$ for the stationary sample and the highest mean of 402.08 $\mu g\,m^{-3}$ for a personal sample that was positioned on the collar of the researcher standing close to the stationary sample. Burn 5 showed the second highest black carbon value of 218.58 $\mu g\,m^{-3}$ for the personal sampler that was fitted to the researcher walking around the field during the burn. This value was significantly higher than those reported for the other samples, which indicates that personal exposure can be minimized by the position of the worker during the burn event. The black carbon values correlated well with total PAHs (correlation coefficient [r] = 0.91 as per Supporting Information, Figure S2), with Burns 2 and 5 showing significantly higher concentrations of both PAHs and black carbon. The higher black carbon values are also indicative of more smoke during the burn and thus more incomplete combustion; therefore monitoring of black carbon provides a complementary tool to the monitoring of PAHs.

CONCLUSIONS

The sugar cane industry represents a vital portion of the South African economy, but the adverse environmental implications of preharvest practices need to be well understood, due to the atmospheric air pollutants emitted during biomass burning. These raise health concerns not only for the workers who are on site during the burn but also to rural and urban populations in the vicinity. In our study, gas and particulate PAHs were simultaneously determined, for the first time in South Africa, for different preharvest burn events at five different sites in the Kwa-Zulu Natal Province. Small portable denuder devices were successfully employed for sampling; these offer advantages over conventional methods in that they minimize sampling artifacts and avoid time-consuming and environmentally unfriendly sample preparation techniques. They are also readily portable and give additional insight into atmospheric partitioning. During preharvest sugar cane burns, the individual and total PAH concentrations, ranging from two-ring naphthalene to four-ring pyrene, increased up to 10 times compared with upwind samples, and over 90% of the overall total PAHs, equating to 17.20 $\mu g\,m^{-3}$, were found to exist in the gas phase and 1.68 $\mu g\,m^{-3}$ in the particulate phase. This is a significant finding because the smaller, gas phase PAHs, which have higher vapor pressures, undergo atmospheric oxidative

TABLE 5: Mean and median equivalent black carbon concentrations determined via aethalometer readings during different sugar cane burn events

	Stationary samples		Personal sampler 1		Personal sampler 2		Personal sampler 3	
Burn no.	Mean ($\mu g\,m^{-3}$)	Median ($\mu g\,m^{-3}$)	Mean ($\mu g\,m^{-3}$)	Median ($\mu g\,m^{-3}$)	Mean ($\mu g\,m^{-3}$)	Median ($\mu g\,m^{-3}$)	Mean ($\mu g\,m^{-3}$)	Median ($\mu g\,m^{-3}$)
Burn 1	18.06	4.04	41.01	22.26	21.96	7.37	6.34	2.98
Burn 2	430.91	125.53	269.30	154.95	166.31	26.68	402.08	282.19
Burn 3	40.41	3.78	23.33	2.36	18.58	2.07	22.58	2.71
Burn 4	0.91	1.07	8.01	1.22	2.48	2.42	<LOQ	<LOQ
Burn 5	1.90	1.45	1.77	1.59	3.03	3.06	218.58	8.58

Conditional formatting color scales were employed for visual effect, with red indicating the highest and green indicating the lowest concentrations.
eBC = equivalent black carbon; LOQ = limit of quantitation.

gas-to-particle conversions and multiphase aging reactions and contribute to the toxicity of generated secondary organic aerosols (Offer et al., 2022). The PAH fingerprints were significantly different between each burn event, indicating the vital role that prevailing weather conditions as well as the nature of the burn and the crop play in emissions and the gas-particle partitioning thereof. The lowest total and individual PAH emissions were found for the burn event that was the most contained and rapid where there was no recorded wind.

It is recommended that the method employed be further optimized, specifically the method for desorption of PAHs from the QFF for the accurate quantification of heavier PAHs, which have higher toxicity. Further investigations should be conducted to better elucidate PAH phase partitioning, with an emphasis on transient phase associations in the fresh emissions to gain a better understanding of the role that atmospheric conditions such as ambient temperature and relative humidity may play. In this regard, a large sample set would be needed to demonstrate statistically significant correlations between a large number of variables, to form definitive conclusions. Atmospheric aging can result in the formation of toxic PAH derivatives due to chemical oxidation of primary gaseous PAHs, and because low-molecular-weight gas phase PAHs were found to be more abundant in our study, it would be valuable to characterize and quantify these derivatives as well as secondary organic aerosols resulting from the condensation of gas phase PAHs onto particles.

The findings of our study suggest that the determination of PM alone would lead to a gross underestimation of potential environmental and human health impacts and therefore gas phase PAH pollutants should be included when conducting risk assessments and considering control strategies. Although the burn events described in our study are performed in accordance with industry regulations, the present study may aid in further optimizing the burn conditions to ensure complete combustion and thus fewer PAH emissions, as seen during still conditions with a more contained and fast burn. Our study can aid in the determination of best practice in sugar cane harvesting toward enhancing greater sustainability. One consideration in this respect is the exploration of a combustion alternative and the conversion of biomass waste into biofuels, while simultaneously minimizing the emission of harmful air pollutants.

Supporting Information—The Supporting Information is available on the Wiley Online Library at https://doi.org/10.1002/etc.5579.

Acknowledgments—The Department of Chemistry at the University of Pretoria as well as Impala Platinum are acknowledged for their support and resources. The Helmholtz Zentrum, Helmholtz International Lab aeroHEALTH and the Federal Ministry of Education and Research (BMBF) in Germany are also duly acknowledged, with special thanks to the Comprehensive Molecular Analytics (CMA) group at Helmholtz Zentrum München. LECO is acknowledged for the use of ChromaTOF Tile software. Funding provided by the University of Pretoria, Impala Platinum, and the National Research Foundation of South Africa (grant 105877) is acknowledged. Our research was supported by the Helmholtz Association/Berlin and the BMBF, research contract 01DG17023.

Disclaimer—The authors declare no conflict of interest.

Author Contributions Statement—**G. Geldenhuys**: Methodology; Validation; Formal analysis; Data curation; Writing—original draft and review & editing. **J. Orasche**: Methodology; Formal analysis; Writing—review & editing. **G. Jakobi**: Methodology; Formal analysis; Writing—review & editing. **Ralf Zimmermann**: Conceptualization; Writing—review & editing; Funding acquisition. **P.B.C. Forbes**: Conceptualization; Visualization; Project administration; Methodology; Formal analysis; Writing—review & editing; Funding acquisition.

Data Availability Statement—All associated data and calculation tools are available in the Supporting Information or directly from the corresponding author (patricia.forbes@up.ac.za).

REFERENCES

Amarillo, A. C., & Carreras, H. (2016). Quantifying the influence of meteorological variables on particle-bound PAHs in urban environments. *Atmospheric Pollution Research*, *7*(4), 597–602.

Breuer, D. (2010). Analytical performance issues: GESTIS database: International limit values for chemical agents—A readily accessible source of Occupational Exposure Limits (OELs). *Journal of Occupational and Environmental Hygiene*, *7*(7), D37–D42.

Chen, J., Li, C., Ristovski, Z., Milic, A., Gu, Y., Islam, M. S., & He, C. (2017). A review of biomass burning: Emissions and impacts on air quality, health and climate in China. *Science of the Total Environment*, *579*, 1000–1034.

Climate-Data.org. (nd). Climate: Kwazulu-Natal. https://en.climate-data.org/africa/south-africa/kwazulu-natal

Dat, N.-D., & Chang, M. B. (2017). Review on characteristics of PAHs in atmosphere, anthropogenic sources and control technologies. *Science of the Total Environment*, *609*, 682–693.

de Andrade, S. J., Cristale, J., Silva, F. S., Zocolo, G. J., & Marchi, M. R. (2010). Contribution of sugar-cane harvesting season to atmospheric contamination by polycyclic aromatic hydrocarbons (PAHs) in Araraquara city, Southeast Brazil. *Atmospheric Environment*, *44*(24), 2913–2919.

Delistraty, D. (1997). Toxic equivalency factor approach for risk assessment of polycyclic aromatic hydrocarbons. *Toxicological & Environmental Chemistry*, *64*(1-4), 81–108.

Dragan, G. C., Kohlmeier, V., Orasche, J., Schnelle-Kreis, J., Forbes, P. B., Breuer, D., & Zimmermann, R. (2020). Development of a personal aerosol sampler for monitoring the particle–vapour fractionation of SVOCs in workplaces. *Annals of Work Exposures and Health*, *64*(8), 903–908.

Elorduy, I., Elcoroaristizabal, S., Durana, N., García, J. A., & Alonso, L. (2016). Diurnal variation of particle-bound PAHs in an urban area of Spain using TD-GC/MS: Influence of meteorological parameters and emission sources. *Atmospheric Environment*, *138*, 87–98.

Flack-Prain, S., Shi, L., Zhu, P., da Rocha, H. R., Cabral, O., Hu, S., & Williams, M. (2021). The impact of climate change and climate extremes on sugarcane production. *GCB Bioenergy*, *13*(3), 408–424.

Forbes, P. (2015). *Monitoring of air pollutants: Sampling,sample preparation and analytical techniques* (Vol. *70*). Elsevier.

Forbes, P. B., Karg, E. W., Zimmermann, R., & Rohwer, E. R. (2012). The use of multi-channel silicone rubber traps as denuders for polycyclic aromatic hydrocarbons. *Analytica Chimica Acta*, *730*, 71–79.

Forbes, P. B., & Rohwer, E. R. (2009). Investigations into a novel method for atmospheric polycyclic aromatic hydrocarbon monitoring. *Environmental Pollution*, *157*(8-9), 2529–2535.

Geldenhuys, G., Rohwer, E. R., Naudé, Y., & Forbes, P. B. (2015). Monitoring of atmospheric gaseous and particulate polycyclic aromatic hydrocarbons in South African platinum mines utilising portable denuder sampling with analysis by thermal desorption–comprehensive gas chromatography–mass spectrometry. *Journal of Chromatography A*, *1380*, 17–28.

Godoi, A. F., Ravindra, K., Godoi, R. H., Andrade, S. J., Santiago-Silva, M., Van Vaeck, L., & Van Grieken, R. (2004). Fast chromatographic determination of polycyclic aromatic hydrocarbons in aerosol samples from sugar cane burning. *Journal of Chromatography A*, *1027*(1-2), 49–53.

Hall, D., Wu, C.-Y., Hsu, Y.-M., Stormer, J., Engling, G., Capeto, K., Wang, J., Brown, S., Li, H.-W., & Yu, K.-M. (2012). PAHs, carbonyls, VOCs and PM2. 5 emission factors for pre-harvest burning of Florida sugarcane. *Atmospheric Environment*, *55*, 164–172.

Keith, L. H. (2015). The source of U.S. EPA's sixteen PAH priority pollutants. *Polycyclic Aromatic Compounds*, *35*(2-4), 147–160. https://doi.org/10.1080/10406638.2014.892886

Keyte, I. J., Albinet, A., & Harrison, R. M. (2016). On-road traffic emissions of polycyclic aromatic hydrocarbons and their oxy-and nitro-derivative compounds measured in road tunnel environments. *Science of the Total Environment*, *566*, 1131–1142.

Kohlmeier, V., Dragan, G. C., Karg, E. W., Schnelle-Kreis, J., Breuer, D., Forbes, P. B., & Zimmermann, R. (2017). Multi-channel silicone rubber traps as denuders for gas–particle partitioning of aerosols from semi-volatile organic compounds. *Environmental Science: Processes & Impacts*, *19*(5), 676–686.

Kumari, K. M., & Lakhani, A. (2018). PAHs in gas and particulate phases: Measurement and control. In T. Gupta, A. K. Agarwal, R. A. Argarwal, & N. K. Labhsetwar (Eds.), *Environmental contaminants* (pp. 43–75). Springer.

Kural, G., Balkis, N. C., & Abdullah, A. K. S. U. (2018). Source identification of polycyclic aromatic hydrocarbons (PAHs) in the urban environment of Istanbul. *International Journal of Environment and Geoinformatics*, *5*(1), 53–67.

Li, X., Yang, Y., Xu, X., Xu, C., & Hong, J. (2016). Air pollution from polycyclic aromatic hydrocarbons generated by human activities and their health effects in China. *Journal of Cleaner Production*, *112*, 1360–1367.

Masih, J., Singhvi, R., Taneja, A., Kumar, K., & Masih, H. (2012). Gaseous/particulate bound polycyclic aromatic hydrocarbons (PAHs), seasonal variation in North central part of rural India. *Sustainable Cities and Society*, *3*, 30–36.

Mugica-Álvarez, V., Hernández-Rosas, F., Magaña-Reyes, M., Herrera-Murillo, J., Santiago-De La Rosa, N., Gutiérrez-Arzaluz, M., & González-Cardoso, G. (2018). Sugarcane burning emissions: Characterization and emission factors. *Atmospheric Environment*, *193*, 262–272.

Mugica-Alvarez, V., Santiago-de la Rosa, N., Figueroa-Lara, J., Flores-Rodríguez, J., Torres-Rodríguez, M., & Magaña-Reyes, M. (2015). Emissions of PAHs derived from sugarcane burning and processing in Chiapas and Morelos México. *Science of the Total Environment*, *527*, 474–482.

Munyeza, C. F., Kohlmeier, V., Dragan, G. C., Karg, E. W., Rohwer, E. R., Zimmermann, R., & Forbes, P. B. (2019). Characterisation of particle collection and transmission in a polydimethylsiloxane based denuder sampler. *Journal of Aerosol Science*, *130*, 22–31.

Nadali, A., Leili, M., Bahrami, A., Karami, M., & Afkhami, A. (2021). Phase distribution and risk assessment of PAHs in ambient air of Hamadan, Iran. *Ecotoxicology and Environmental Safety*, *209*, 111807.

Nisbet, I. C., & Lagoy, P. K. (1992). Toxic equivalency factors (TEFs) for polycyclic aromatic hydrocarbons (PAHs). *Regulatory Toxicology and Pharmacology*, *16*(3), 290–300.

Offer, S., Hartner, E., Di Bucchianico, S., Bisig, C., Bauer, S., Pantzke, J., & Zimmermann, R. (2022). Effect of atmospheric aging on soot particle toxicity in lung cell models at the air–liquid interface: Differential toxicological impacts of biogenic and anthropogenic secondary organic aerosols (SOAs). *Environmental Health Perspectives*, *130*(2), 027003.

Pandey, S. K., Kim, K.-H., & Brown, R. J. (2011). A review of techniques for the determination of polycyclic aromatic hydrocarbons in air. *TrAC, Trends in Analytical Chemistry*, *30*(11), 1716–1739.

Poster, D. L., Schantz, M. M., Sander, L. C., & Wise, S. A. (2006). Analysis of polycyclic aromatic hydrocarbons (PAHs) in environmental samples: A critical review of gas chromatographic (GC) methods. *Analytical and Bioanalytical Chemistry*, *386*(4), 859–881. https://doi.org/10.1007/s00216-006-0771-0

Pryor, S. W., Smithers, J., Lyne, P., & van Antwerpen, R. (2017). Impact of agricultural practices on energy use and greenhouse gas emissions for South African sugarcane production. *Journal of Cleaner Production*, *141*, 137–145.

PubChem. (2021). PubChem Database. https://pubchem.ncbi.nlm.nih.gov/compound

Rengarajan, T., Rajendran, P., Nandakumar, N., Lokeshkumar, B., Rajendran, P., & Nishigaki, I. (2015). Exposure to polycyclic aromatic hydrocarbons with special focus on cancer. *Asian Pacific Journal of Tropical Biomedicine*, *5*(3), 182–189.

Rezaei, F., Kakooei, H., Ahmadkhaniha, R., Azam, K., Omidi, L., & Shahtaheri, S. J. (2015). Personal exposure to polycyclic aromatic hydrocarbons in newsagents in Tehran, Iran. *Iranian Journal of Public Health*, *44*(5), 665.

Samae, H., Tekasakul, S., Tekasakul, P., & Furuuchi, M. (2021). Emission factors of ultrafine particulate matter (PM < 0.1 μm) and particle-bound polycyclic aromatic hydrocarbons from biomass combustion for source apportionment. *Chemosphere*, *262*, 127846.

Sevimoglu, O., & Rogge, W. F. (2016). Seasonal size-segregated PM10 and PAH concentrations in a rural area of sugarcane agriculture versus a coastal urban area in Southeastern Florida, USA. *Particuology*, *28*, 52–59.

Sevimoğlu, O., & Rogge, W. F. (2019). Seasonal variations of PM10—Trace elements, PAHs and Levoglucosan: Rural sugarcane growing area versus coastal urban area in Southeastern Florida, USA. Part II: Elemental concentrations. *Particuology*, *46*, 99–108.

Schnelle-Kreis, J., Sklorz, M., Peters, A., Cyrys, J., & Zimmermann, R. (2005). Analysis of particle-associated semi-volatile aromatic and aliphatic hydrocarbons in urban particulate matter on a daily basis. *Atmospheric Environment*, *39*(40), 7702–7714.

Schnelle-Kreis, J., Welthagen, W., Sklorz, M., & Zimmermann, R. (2005). Application of direct thermal desorption gas chromatography and comprehensive two-dimensional gas chromatography coupled to time of flight mass spectrometry for analysis of organic compounds in ambient aerosol particles. *Journal of Separation Science*, *28*(14), 1648–1657.

Sharma, H., Jain, V., & Khan, Z. H. (2007). Characterization and source identification of polycyclic aromatic hydrocarbons (PAHs) in the urban environment of Delhi. *Chemosphere*, *66*(2), 302–310.

Solomon, S. (2011). Sugarcane by-products based industries in India. *Sugar Tech: An International Journal of Sugar Crops and Related Industries*, *13*(4), 408–416. https://doi.org/10.1007/s12355-011-0114-0

South African Sugar Association (SASA). (2012). S.A. Sugar Association, Mount Edgecombe.

South African Sugar Association. (2019). The South African Sugar Industry Directory 2019/2020 Report. https://sasa.org.za/custom_content/downloads/SASA-ID-2019-20.pdf

South African Sugarcane Research Institute. (2022). Farms located throughout SA sugar belt. https://sasri.org.za/variety-improvement/

Tan, J.-H., Bi, X.-H., Duan, J.-C., Rahn, K. A., Sheng, G.-Y., & Fu, J.-M. (2006). Seasonal variation of particulate polycyclic aromatic hydrocarbons associated with PM10 in Guangzhou, China. *Atmospheric Research*, *80*(4), 250–262.

Tan, J., Guo, S., Ma, Y., Duan, J., Cheng, Y., He, K., & Yang, F. (2011). Characteristics of particulate PAHs during a typical haze episode in Guangzhou, China. *Atmospheric Research*, *102*(1-2), 91–98.

Vione, D., Barra, S., de Gennaro, G., de Rienzo, M., Gilardoni, S., Perrone, M. G., & Pozzoli, L. (2004). Polycyclic aromatic hydrocarbons in the atmosphere: Monitoring, sources, sinks and fate. II: Sinks and fate. *Annali di Chimica*, *94*(4), 257–268. https://doi.org/10.1002/adic.200490031

Zamperlini, G., Silva, M., & Vilegas, W. (1997). Identification of polycyclic aromatic hydrocarbons in sugar cane soot by gas chromatography-mass spectrometry. *Chromatographia*, *46*(11-12), 655–663.

